



## Serially Deposited Amorphous Aggregates of Hard Spheres

Charles H. Bennett

Citation: *J. Appl. Phys.* **43**, 2727 (1972); doi: 10.1063/1.1661585

View online: <http://dx.doi.org/10.1063/1.1661585>

View Table of Contents: <http://jap.aip.org/resource/1/JAPIAU/v43/i6>

Published by the [American Institute of Physics](#).

---

### Additional information on J. Appl. Phys.

Journal Homepage: <http://jap.aip.org/>


Journal Information: [http://jap.aip.org/about/about\\_the\\_journal](http://jap.aip.org/about/about_the_journal)

Top downloads: [http://jap.aip.org/features/most\\_downloaded](http://jap.aip.org/features/most_downloaded)

Information for Authors: <http://jap.aip.org/authors>

## ADVERTISEMENT

**World's Ultimate AFM** Experience the Speed & Resolution



**The fastest AFM on the planet is now simply the best AFM in the world**

[CLICK TO REQUEST INFO](#)

In this result  $y'_0(0)/y_0(0)$  is given in terms of gamma functions by Eq. (50). For large  $k$  we have

$$\delta = (23)^{1/2}/4, \quad (89)$$

and the use of Stirling's formula for the gamma function gives

$$y'_0(0)/y_0(0) = \frac{1}{2}(23)^{1/2}. \quad (90)$$

A similar calculation can be carried out in the highly nonspherical case. Omitting the algebraic details, we find as the fraction of the energy in the lower half-space

$$f^- = 2k \left( \frac{E\beta + 1}{2kE\beta + 5k - 1} \right) \left( \frac{5k - 1}{(5k - 1)\alpha E + 2k} \right), \quad (91)$$

with  $\alpha$ ,  $\beta$ , and  $E$  defined by Eqs. (71), (77), and (78). In this case, once  $k$  has been specified, the partition of energy depends upon the single parameter  $E$  rather than the two parameters  $A$  and  $B$  as in Eq. (88). Since  $E$ , defined by Eq. (77), is independent of the densities involved, Eq. (91) shows that the partition of energy is independent of the density ratio of the two half-spaces in the highly nonspherical limit. This dependence of  $f^-$  on  $E$  is shown in Fig. 1 for  $k=7$ , a realistic value for the radiative-transfer problem.<sup>3</sup>

Figure 2 shows typical numerical results calculated from Eq. (88) for  $k=7$ . We have plotted in this figure

the fraction of the energy in the lower half-space ( $f^-$ ) vs the ratio of densities of the two half-spaces ( $R \equiv \rho^-/\rho^+$ ), assuming the other properties of the half-spaces to be identical on a per-unit-mass basis (i.e.,  $\sigma^- = \sigma^+$  and  $\epsilon^- = \epsilon^+$ ). We also show in this figure the large  $R$  limit as given by Eq. (91) with  $E=1$ .

#### ACKNOWLEDGMENT

This work was supported by the U.S. government under contract No. DASA-01-70-C-0140, monitored by the Defense Nuclear Agency.

- <sup>1</sup>R. E. Marshak, *Phys. Fluids* **1**, 24 (1958).
- <sup>2</sup>Ya. Zeldovich and Yu. Raizer, *Physics of Shock Waves and High-Temperature Hydrodynamic Phenomena* (Academic, New York, 1969), Vol. 2, Chap. 10.
- <sup>3</sup>D. E. Parks, *J. Appl. Phys.* **38**, 3369 (1967).
- <sup>4</sup>G. C. Pomraning, *J. Appl. Phys.* **38**, 3845 (1967).
- <sup>5</sup>G. C. Pomraning, *J. Appl. Phys.* **39**, 1479 (1968).
- <sup>6</sup>C. Wagner, *J. Chem. Phys.* **18**, 1227 (1950).
- <sup>7</sup>L. Weisberg and J. Blanc, *Phys. Rev.* **131**, 1548 (1963).
- <sup>8</sup>W. Kass and M. O'Keefe, *J. Appl. Phys.* **37**, 2377 (1966).
- <sup>9</sup>T. Marx, W. Snyder, A. St. John, and C. Moeller, *J. Appl. Physiol.* **15**, 1123 (1960).
- <sup>10</sup>I. Fatt and T. Goldstick, *J. Colloid Sci.* **20**, 962 (1965).
- <sup>11</sup>R. H. Boyer, Westinghouse Scientific Paper No. 10-1210-5-P4, 1959 (unpublished).
- <sup>12</sup>H. Fujita, *Textile Res. J.* **22**, 757 (1952).
- <sup>13</sup>H. Fujita, *Textile Res. J.* **22**, 823 (1952).
- <sup>14</sup>E. I. Andriankin, *Sov. Phys. JETP* **35**, 428 (1958).

## Serially Deposited Amorphous Aggregates of Hard Spheres\*

Charles H. Bennett<sup>†</sup>

Harvard University, Cambridge, Massachusetts 02138

and

Argonne National Laboratory, Argonne, Illinois 60439

(Received 20 August 1971)

Aggregates of several thousand equal hard spheres were constructed by depositing additional spheres, one at a time, at surface sites on a small seed cluster, placing each new sphere in contact with three already present and not moving it afterward. Always choosing the site closest to the center of the original seed results in an aggregate showing no evidence of crystallinity, with a pair correlation function quite similar to that of the dense random packings which have been prepared from ball bearings, and to the pair correlation functions calculated from x-ray diffraction work on amorphous alloys. The packing density  $\frac{1}{6} \pi N \sigma^3/V$  and the mean coordination number both decrease with distance from the center; the large-aggregate limits are, respectively, 0.61 (extrapolated, 4% lower than the ball-bearing value), and exactly 6.0 (in agreement with the ball-bearing value). The apparent difficulty of homogeneously nucleating crystallization in hard-sphere systems, even when simultaneous relaxation of many particle positions is allowed, is attributed to the fact that small hcp and fcc fragments are more bulky and have no more hard contacts than amorphous arrangements of the same number of atoms.

### I. INTRODUCTION

The dense random packing<sup>1-3</sup> of equal spheres, which can be prepared in the laboratory by compressing and compacting ball bearings or the like within containers having flexible or irregular walls, was originally proposed as a model of the liquid state, but it now appears to represent more accurately the hypothetical metastable glassy state of simple liquids.<sup>4</sup> This is the state which would be achieved if a simple liquid could be cooled or compressed until the atoms became effectively im-

mobilized without the material's having sustained the growth of a distinct crystal phase.

So far no well-characterized glass has been made from a pure nondirectionally bonded monatomic substance—the usual result is a microcrystalline solid<sup>5</sup>—but many good glasses have been prepared from mixtures of such substances, notably alloys of various noble and transition elements. Amorphous alloys have been produced both by rapid cooling of the melt<sup>6-8</sup> and by techniques, such as vapor deposition<sup>9</sup> and electrodeposition,<sup>10</sup> in

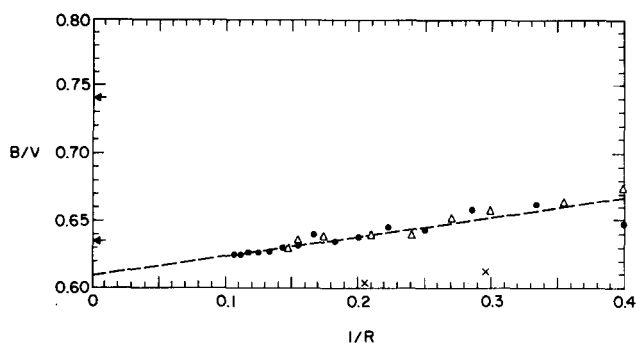


FIG. 1. Size dependence of the mean density of amorphous packings.  $B/V$  is the mean density. Arrows indicate close-packed crystal (0.7405) and Finney's dense random packing density (0.6366).  $R$  is the radius of sphere within which density was measured.  $\Delta$  is the data for 1600-particle cluster packed by global criterion.  $\bullet$  is the data for 3999-particle cluster packed by global criterion.  $\times$  is the data for 1500-particle cluster packed by local criterion.

which atoms are deposited one by one onto a solid substrate from a liquid or gas. In spite of these very different methods of preparation, glasses formed by all these methods resemble each other more than they do liquids or polycrystalline close-packed materials.<sup>10</sup> Characteristically, the pair correlation function has a fairly sharp first peak, a split second peak, and third, fourth, and fifth peaks which are blunt but more pronounced than those found in liquids. As Cargill<sup>10</sup> also points out, the pair correlation functions for alloy glasses are in excellent agreement with those obtained by Finney<sup>3</sup> from a dense random packing of 8000 ball bearings.

The present work explores a mathematically well-defined method for preparing hard-sphere packings on a computer, a method perhaps most analogous to vapor deposition at absolute zero. In general, the method starts with a seed cluster and brings in additional spheres, one at a time, placing each one at a surface site on the existing cluster where it rests in hard contact with three spheres already present. After it has been placed, a sphere is not allowed to move, but becomes part of the substrate upon which subsequent spheres are deposited. It can be seen that the resulting aggregate will be completely determined by (i) the seed cluster and (ii) the criterion by which successive surface sites are chosen for deposition from among the many available at any one time.

Two such criteria were investigated—a “global” criterion in which the new particle was added at the site closest to the center of the original seed cluster,<sup>11</sup> and a “local” criterion in which the new particle was added at the site having the least distance from the plane of its three nearest neighbors.

The global criterion corresponds roughly to choosing the site with the lowest energy in a gravitational or other long-range potential, whereas the local criterion by choosing the deepest “pocket” in which to place the new particle would favor sites most strongly bound by a short-range potential.

Sections II–V describe the three amorphous aggregates which were produced and discuss their packing densities, pair correlation functions, and coordination-number distributions. The results are briefly compared to those obtained from ball-bearing packings, electrodeposited nickel-phosphorus films, and molecular dynamics calculations for the high-density hard-sphere fluid. Sections IV and V discuss issues which bear on amorphous hard-sphere packings generally, namely, their mechanical stability with respect to flow and crystallization and the relation between stability and mean coordination number.

## II. METHODS

The packings were generated by a fairly simple-minded FORTRAN IV program on an IBM 7094 computer. At all times the computer contained lists of the  $x$ ,  $y$ , and  $z$  coordinates for all the particles in the cluster and for all the “pockets” determined by these particles, a pocket being defined as a point lying exactly one particle diameter ( $\sigma$ ) away from each of three particle centers and at least  $\sigma$  away from all the other particle centers in the cluster. In each cycle of operation, the program first selected one of the pockets as the new particle location according to the criteria described above, and

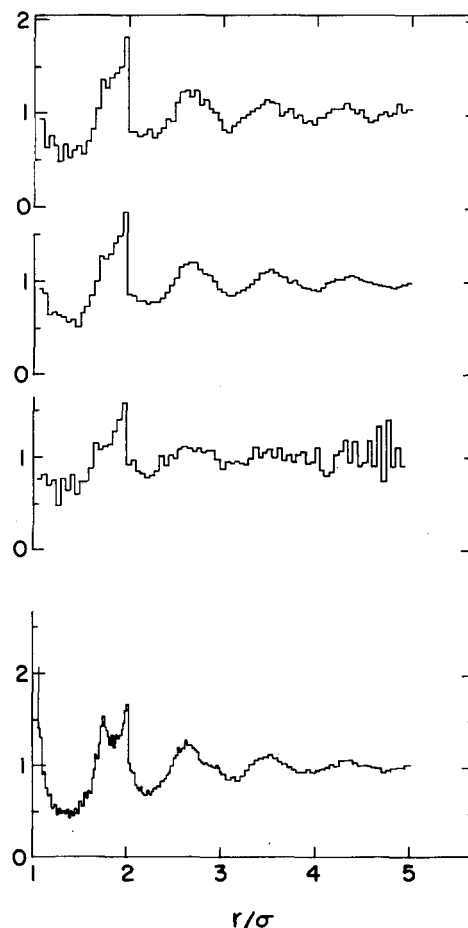


FIG. 2. Pair correlation functions for hard-sphere packings; in order from top curve: 1600-global, 3999-global, 1500-local, and Finney packings.

TABLE I. Pair correlation functions of amorphous packings. Data were collected for 221 centers for the 1600-global, for 485 centers for the 3999-global, and for 209 centers for the 1500-local packing.  $\delta$  is the unit  $\delta$  function  $\delta(R/\sigma - 1)$ .

$R/\sigma$	1600 global	3999 global	1500 local	$R/\sigma$	1600 global	3999 global	1500 local
1.000	0.588	0.478	0.478				
1.025	...	2.28	...	3.025	0.84	0.90	0.86
1.075	0.95	0.93	0.75	3.075	0.81	0.87	0.94
1.125	0.64	0.88	0.82	3.125	0.88	0.87	0.93
1.175	0.77	0.65	0.68	3.175	0.91	0.89	0.95
1.225	0.65	0.67	0.74	3.225	0.96	0.92	0.94
1.275	0.49	0.64	0.48	3.275	0.99	0.96	0.93
1.325	0.67	0.63	0.76	3.325	1.03	0.98	0.98
1.375	0.52	0.57	0.63	3.375	1.07	1.05	1.10
1.425	0.62	0.60	0.80	3.425	1.10	1.11	1.00
1.475	0.66	0.51	0.59	3.475	1.14	1.12	1.05
1.525	0.57	0.66	0.74	3.525	1.14	1.14	1.08
1.575	0.71	0.74	0.74	3.575	1.11	1.11	0.99
1.625	0.83	0.86	0.87	3.625	0.99	1.07	1.09
1.675	1.06	1.01	1.14	3.675	1.01	1.06	0.96
1.725	1.37	1.28	1.08	3.725	1.05	1.00	1.03
1.775	1.26	1.25	1.12	3.775	0.95	1.02	0.95
1.825	1.38	1.30	1.14	3.825	0.99	0.97	1.03
1.875	1.43	1.43	1.27	3.875	0.92	0.95	1.06
1.925	1.50	1.50	1.40	3.925	0.93	0.94	0.94
1.975	1.82	1.76	1.57	3.975	0.89	0.93	0.95
2.025	0.80	0.87	0.92	4.025	0.96	0.92	1.11
2.075	0.80	0.86	0.97	4.075	0.96	0.95	0.87
2.125	0.76	0.80	0.85	4.125	1.02	1.00	0.80
2.175	0.77	0.79	0.83	4.175	1.05	1.01	0.84
2.225	0.83	0.78	0.78	4.225	1.05	1.04	1.02
2.275	0.75	0.78	0.81	4.275	1.05	1.04	1.06
2.325	0.79	0.79	0.84	4.325	1.12	1.08	1.18
2.375	0.84	0.83	1.00	4.375	1.06	1.08	0.94
2.425	0.93	0.89	0.91	4.425	1.00	1.07	1.17
2.475	0.93	0.97	1.01	4.475	1.04	1.04	0.91
2.525	1.11	1.05	0.99	4.525	0.97	1.02	0.95
2.575	1.24	1.17	1.09	4.575	0.91	1.01	1.19
2.625	1.24	1.19	1.10	4.625	0.93	0.99	0.90
2.675	1.17	1.21	1.09	4.675	1.00	0.98	1.33
2.725	1.25	1.21	1.05	4.725	1.02	0.97	0.74
2.775	1.08	1.14	1.10	4.775	0.97	0.96	1.39
2.825	1.16	1.10	1.05	4.825	1.00	0.95	0.89
2.875	1.06	1.09	1.06	4.875	1.10	0.96	1.11
2.925	1.02	1.01	1.06	4.925	1.01	0.98	0.91
2.975	0.93	0.93	0.98	4.975	1.04	0.99	0.73

then updated the pocket list. This updating, which consumed the bulk of the computing time, consisted of deleting from the pocket list the selected pocket and all other pockets overlapped by the new particle, and then adding to it all the new pockets defined by the new particle in conjunction with pairs of particles already present. Since particles with a center-to-center distance of more than  $2\sigma$  cannot participate in forming the same pocket, the calculation of new pockets was done using a restricted list of particles within this distance of the newly added particle. Input consisted of the seed cluster with its pockets. The program required about  $\frac{1}{2}$  h to build a cluster of 4000 particles.

The seed used in all runs was an equilateral triangle of three particles in contact. Two runs were made using the global (closest to the origin) criterion; in one the origin was placed at the center of one of the particles, and in the other at a point of contact between two. Deposition was continued to a total of 1600 and 3999

particles, respectively. A third cluster of 1500 particles was generated using the local (coplanarity) criterion which does not depend on the coordinate origin.

Except in the immediate neighborhood of the seed, the locations of the deposited particles were completely different in all three runs. However, the two runs using the global criterion were remarkably similar in their statistical properties (e.g., density, pair correlation function, etc.), and as expected both were spherical and centered at the origin. The local-criterion packing was a roughly egg-shaped body with a center of gravity about  $5\sigma$  from the original seed and had statistical properties quite different from the other two packings.

Except near the seed, all packings lacked microscopic symmetry, e.g., taking point  $\mathbf{r}$  as the location of a particle center, and  $\mathbf{r}'$  as the reflection of  $\mathbf{r}$  in one of the seed's planes of symmetry, there would typically be no particle center at point  $\mathbf{r}'$ . The asymmetry originates

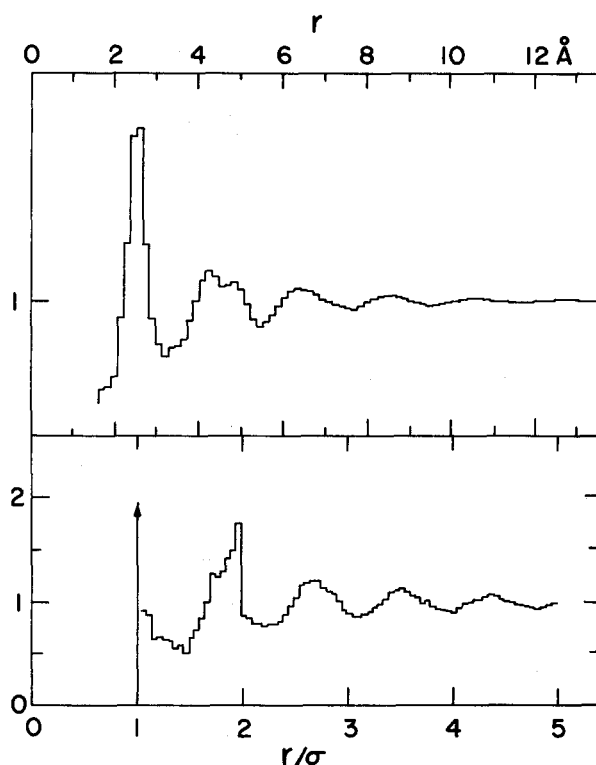


FIG. 3. Pair correlation functions of electrodeposited Ni-P film (upper curve) and 3999-global cluster. Relative scale is  $\sigma = 2.5 \text{ \AA}$ .

when the program is faced with two or more equally desirable pockets and must decide on the basis of roundoff errors and the like which one to fill first. The macroscopic asymmetry of the local-packing results in the same way when, after depositing about six particles at equivalent regular-tetrahedral sites, the program deposits a particle which interferes with the preceding particles and defines a pocket whose base is not an equilateral triangle. Such an "irregular" pocket is preferred by the local criterion to the preceding regular pockets because its altitude above the base triangle is less than that of a regular tetrahedron, and, since the filling of one irregular pocket always generates at least one new irregular pocket, the program never returns to fill the remaining regular pockets. Thus, after an initial period of symmetric growth, a spurt of growth takes place at one end of the cluster, completely destroying its symmetry and displacing the center of gravity.

Although no other seeds were studied, a few inferences can be made about the probable effect of varying the seed, at least in the case of the global criterion. The statistical similarity of the two global clusters and the fact that at each stage of growth the existing cluster serves as the seed for subsequent growth suggest that almost any small or amorphous seed would, under the global criterion, yield a cluster statistically similar to the two that have been made. A fcc or hcp crystalline seed would probably not be able to grow in all directions without developing stacking faults or grain boundaries, or perhaps even amorphous regions, under the global criterion, because the spherically growing crystal could not help exposing crystallographic planes

dense enough to have overlapping sets of pockets (e.g., a close-packed plane has twice as many pockets as can be occupied by the next atomic layer), and the program would sometimes make wrong choices. This inability to build a good crystal has no physical significance, since it is a consequence of the absolute and unrealistic immobility of particles once they have been deposited.

### III. DENSITY

Density, the ratio of the total volume of a number of spheres,  $B = \frac{1}{6} N \sigma^3 \pi$ , to the volume  $V$  containing them, was calculated by counting the number of centers in as large a spherical region as could be contained entirely within the cluster. The highest over-all density achieved by any space-filling packing of equal spheres is  $B/V = \frac{1}{6} (2^{1/2} \pi) = 0.7405$  for the fcc and hcp crystals; the density of Finney's ball-bearing packing is  $0.6366 \pm 0.0004$ . Of the present packings, the two constructed using the global criterion yielded densities between 0.62 and 0.63, while the one using the local criterion had a density of about 0.60.

As Fig. 1 shows, density decreases with increasing cluster size. A linear extrapolation versus the reciprocal of the cluster radius yields a limiting density of about 0.61 for an infinite cluster packed by the global criterion, and a considerably lower limiting value, about 0.57, for the local criterion. Since the loosest of the random packings made by Bernal and Scott exceeded this bulk density, it is probable that the computer packing generated by the local criterion is mechanically unstable and, hence, probably a poor model for amorphous solids produced in the laboratory.

The density  $B/V$  is obviously somewhat ill-defined for real materials composed of atoms lacking a hard core. However, by fitting his pair correlation function for electrodeposited Ni-P to Finney's for ball bearings, Cargill<sup>10</sup> obtains an effective packing density of 0.669 for the Ni-P.

### IV. PAIR CORRELATION FUNCTION

The pair correlation function was calculated from the particle coordinates in the usual manner, averaging over several hundred centers near the middle of the cluster. Knowledge of the pocket coordinates allowed the program to detect the cluster's periphery and to avoid looking for particles in any spherical shell not entirely within the cluster. This function, denoted  $g(r)$ , expresses the frequency of particle pairs separated by a distance  $r$ , relative to the frequency which would be expected in a

TABLE II. Maxima of the pair correlation function for serially deposited clusters, Finney's dense random packing, and Cargill's electrodeposited Ni-P films.

System	$R/\sigma$ values at successive maxima					
1500 local	1.00	1.67 <sub>3</sub>	2.00	...	...	...
3999 global	1.00	1.73 <sub>3</sub>	2.00	2.68 <sub>3</sub>	3.53 <sub>3</sub>	4.38 <sub>3</sub>
Finney dense random packing	1.00	1.73	2.00	2.65	3.50 <sub>3</sub>	4.35 <sub>3</sub>
Ni-P <sup>a</sup>	1.05	1.74	2.00	2.65	3.52	4.35

<sup>a</sup> Effective hard-sphere diameter taken to be  $2.42 \text{ \AA}$  for best fit.

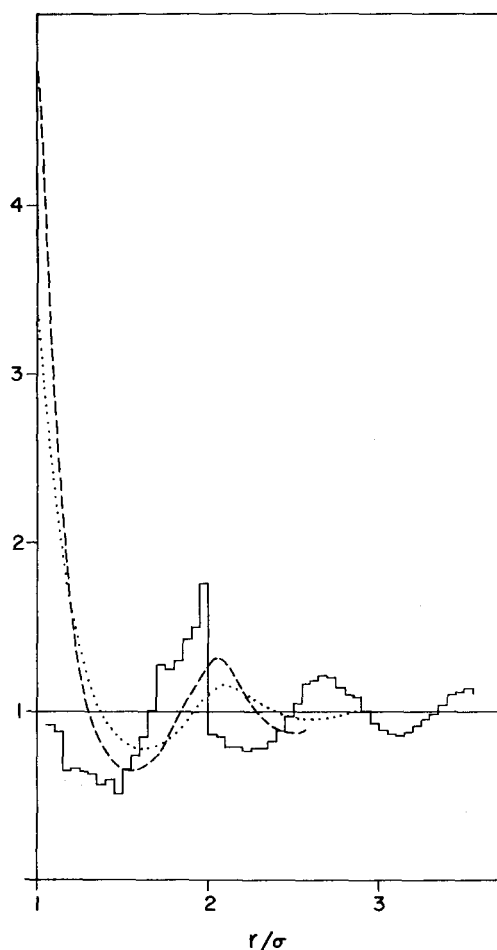


FIG. 4. Pair correlation functions of 3999-global cluster (histogram), hard-sphere fluid at  $B/V=0.37$  (dotted line), and hard-sphere fluid at  $B/V=0.445$  (dashed line).

random array of points with the same number density; it is tabulated for all three serial packings in Table I. In Fig. 2 the pair correlation functions of the computer-generated clusters are compared with that of Finney's packing. The two clusters obtained by the global criterion are in excellent agreement with each other and in good agreement with Finney's packing, which differs mainly in having a more pronounced peak at  $r/\sigma=\sqrt{3}$ . However, in the pair correlation for the local-criterion cluster, the oscillations about unity are much weaker, and the shoulder on the second peak is at 1.65–1.70 rather than in the interval including  $\sqrt{3}$ .

Cargill<sup>10</sup> has pointed out the similarity of Finney's pair correlation function to those of his electrodeposited Ni-P alloys (and indeed to those of most other amorphous alloys, whether formed by homogeneous cooling or heterogeneous deposition). The principal discrepancy between the Ni-P and dense random pair correlation functions (PCF's) is that, if the effective hard-sphere diameter is chosen for best over-all fit between the two curves ( $\sigma=2.42$  Å), the first peak in the Ni-P curve is about 5% farther out, 2.53 Å, than the  $\delta$  function of the hard-sphere curve. The same is true of the comparison between Ni-P and the present computer packings done

using the global criterion. Figure 3 compares a Ni-P PCF with that of the larger global-criterion cluster, and Table II compares the positions of the maxima in these and Finney's PCF.

Perhaps the best way to see the effect of vitrification on the PCF is to compare Finney's (or the author's) PCF with that of a high-density hard-sphere fluid, in which the particles are not jammed tightly against one another, since presumably the high-density limit of the hard-sphere fluid would be a dense random structure similar to the ball-bearing packings. The hard-sphere fluid PCF may be calculated approximately by the Percus-Yevick equation, or it may be obtained directly by averaging over the configurations generated by a molecular dynamics or Monte Carlo calculation. Figure 4 compares the PCF for the larger global packing ( $B/V=0.62$ ) with those of a hard-sphere fluid at densities  $B/V=0.37$  (dotted line) and 0.445 (dashed line) obtained by a molecular dynamics calculation.<sup>12</sup> The progressive development, with increasing density, of the characteristic features of the dense random packing PCF can be seen—the inward movement of all peaks and minima, the rapid sharpening of the outside of the second peak, and the incipient condensation of the first peak into a  $\delta$  function. No evidence of the peak at  $\sqrt{3}$  occurs at either fluid density. To understand why this peak does not appear until very high density, let us consider what discontinuities in the PCF of the dense random structure ought to be expected simply from the presence of small groups of particles in hard contact. As indicated in Fig. 5(a), a discontinuous drop in the PCF at  $r/\sigma=2$  can be predicted from the inability of an intermediate atom to bridge a gap any wider than this with two hard contacts. Similarly, the continuum of configurations of two hard-bonded equilateral triangles sharing a common side would yield a singularity at

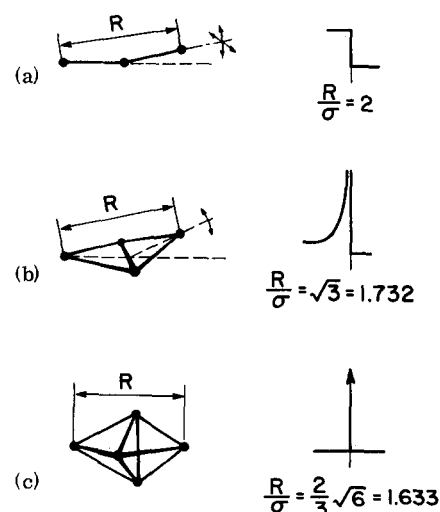


FIG. 5. Simple connected groups of particles and their discontinuous contributions to the pair correlation function. (Two darkened circles connected by a solid line denote two particles in hard contact.)

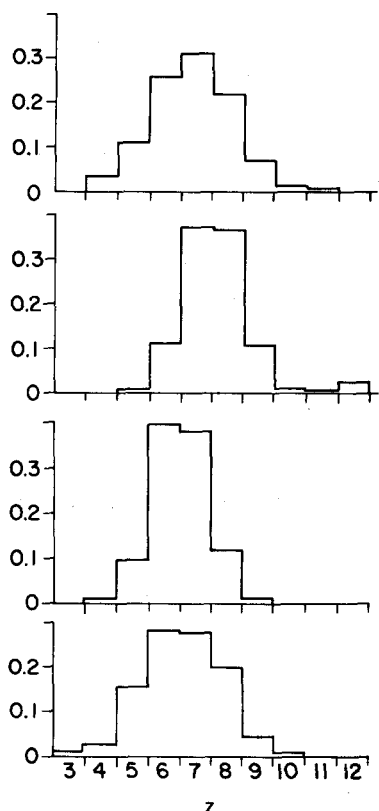


FIG. 6. Distribution of hard-contact coordination numbers  $z$  in hard-sphere packings; in order from the top curve: innermost 209 particles from 1500-local packing, innermost 200 particles from 3999-global packing, particles Nos. 1050-2049 from 3999-global, and Bernal-Mason data for 476 ball bearings.

$r/\sigma = \sqrt{3}$  [Fig. 5(b)]. Since the peak at  $\sqrt{3}$  depends on five hard contacts, it can be no sharper in the fluid than a fifth convolution of the peak at  $r/\sigma = 1$ ; hence, it should only be visible at high density when the first peak is very nearly a  $\delta$  function. Figure 5(c) indicates that occasional trigonal bipyramid configurations ought to yield a  $\delta$ -function singularity at  $(\frac{8}{3})^{1/2} 1.633$ , but this was not detected either in the present work or by Finney, although Finney found a small peak at  $r/\sigma = 1.65$ .

Stillinger<sup>13</sup> considers in more detail connected groups like those shown in Fig. 5, and argues that, if contributions from arbitrarily large groups are included, the resulting singularities in  $g(r)$  are distributed densely along the domain  $r \geq \sigma$ , so that  $g$  is nowhere an analytic function of  $r$ . For the nonjammed fluids Stillinger was considering that these singularities are not discontinuities of  $g$  itself but only of its derivatives (and in most cases only very high-order derivatives). In the high-density limit considered here, each singularity becomes a discontinuity of one of the three types shown in Fig. 5, and  $g$  is nowhere a continuous function of  $r$ . Most of the discontinuities are very weak, and hence even a very good histogram of  $g(r)$  would appear smooth except in a few places, such as  $r/\sigma = 1.0, \sqrt{3}, 2.0$ .

The absence of sharp peaks, either in the present work or in Finney's packings, at the characteristic fcc and

hcp distances, e.g.,  $\sqrt{2}, \sqrt{5}, \sqrt{7}$ , and the smooth oscillations of the PCF beyond  $r/\sigma = 2$  indicate a lack of appreciable crystalline regions. (In the local packing the oscillations damp quickly, and, except for the discontinuities at 1 and 2, the PCF resembles that of a liquid.) Although  $\sqrt{3}$  is a crystal distance also, the observed peak at  $\sqrt{3}$  has been adequately explained above without assuming crystallinity. Since  $\sqrt{2}$  is the body diagonal of a regular octahedron, the absence of a peak at  $\sqrt{2}$  implies a scarcity or absence of perfect and near-perfect octahedra both in the serial packings and in Finney's structure.

#### V. COORDINATION NUMBER, MECHANICAL STABILITY, AND RESISTANCE TO HOMOGENEOUSLY NUCLEATED CRYSTALLIZATION

The mean coordination number at contact, denoted  $\bar{z}$ , was found, like the density, to depend on the size of the cluster. High coordination numbers of 10-12 were found only in the central (oldest) part of the cluster, and with increasing distance from the center the mean coordination number decreased asymptotically toward 6.0. The decrease of  $\bar{z}$  with increasing distance from the seed was most clearcut for the global packings, which remained spherical throughout their growth, but was also present for the more irregularly shaped local packing. Figure 6 gives the coordination number distributions for the innermost 199 particles of the local packing, the innermost 199 particles of the large global packing, 1000 particles near the periphery of the large global packing, and, finally, 476 ball bearings in an early packing of Bernal and Mason.<sup>1</sup> Coordination number distributions for Finney's larger packing have not been calculated, but the mean coordination number is not

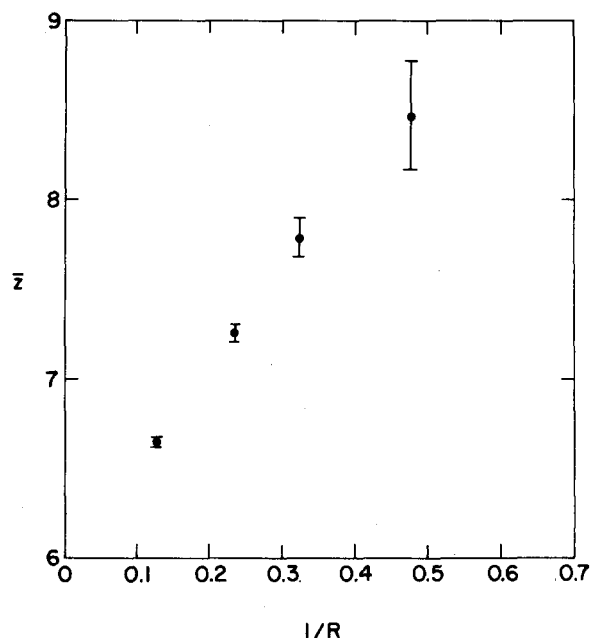


FIG. 7. Radial dependence of local mean coordination number.  $\bar{z}$  is the mean hard-contact number for particles within distance  $R$  of the origin of the 3999-global cluster.

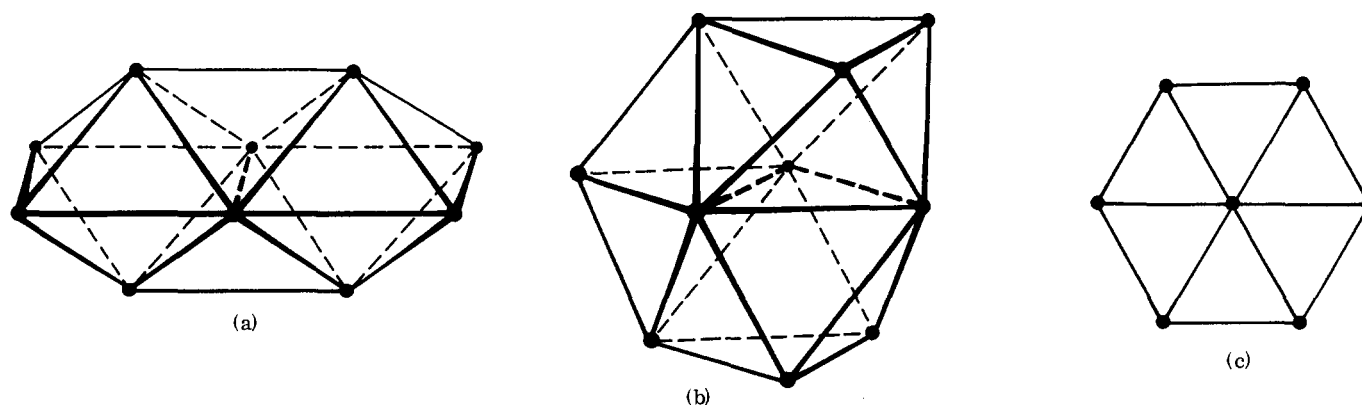


FIG. 8. Minimal aggregates allowing redundant hard contacts in two and three dimensions. Any continuous particle movement leading to one of these configurations will, at the last instant, make contact in several places simultaneously. (a) fcc or hcp fragment (10 particles, 25 contacts), (b) hcp fragment (10 particles, 25 contacts), and (c) two-dimensional hcp fragment (7 particles, 12 contacts).

significantly different from 6.0. The higher value (6.4) found by Bernal and Mason may be due to the small size of the cluster. Figure 7 plots the radial dependence of the coordination number explicitly for the larger global packing,  $\bar{z}$  being averaged over all particles within a distance  $R$  of the origin.

It is easy to see why  $\bar{z}$  should approach 6.0 for large clusters prepared by any one-at-a-time deposition technique, in which each particle rests on three older particles. For any large compactly shaped (e.g., spherical) region within such a cluster, most atoms in the region will only touch other atoms in the region. Since each "bond" between contacting particles has two ends, the mean hard-contact coordination number will be close to 6.0 (three bonds to older atoms and an average of three to younger atoms). Deviation of  $\bar{z}$  from 6.0 will be due to bonds that cross the surface of the region, and hence will decrease as the surface-to-volume ratio if the region is made larger. This approximately linear dependence of the excess coordination number on  $1/R$  is seen in Fig. 7.

A plausible argument, somewhat short of a proof, can be made that the mean coordination for a Bernal-type packing ought also to be 6.0 on account of the relation between mean coordination number and mechanical stability. Suppose that a Bernal-type packing is to be formed by mildly shaking and compressing a cluster originally formed by serial deposition upon a rigid minimally bonded seed (e.g., an equilateral triangle). If the serially deposited cluster contains  $N$  atoms, it will have  $3N-6$  hard contacts which will serve as  $3N-6$  independent constraints on the  $3N$  particle coordinates. The clusters will thus have translational and rotational freedom, but in order for any relative motion of the particles to take place, one or more hard contacts must be broken. During the compacting treatment, hard contacts will be broken and then reformed, and since the particles move along continuous trajectories in time, it is unlikely for more than one new contact to be formed at any one instant. If at a particular instant only one contact is being formed, this contact must

represent an independent constraint on the system's degrees of freedom, since the process of forming a contact involves motion along a degree of freedom which becomes immobilized once contact is made. The number of contacts can only increase above  $3N-6$  if some redundant (i.e., nonindependent) contacts are formed, and, as indicated above, this can only happen if two or more mutually redundant contacts are formed at the same instant, e.g., by the movement of an atom or group of atoms into a precisely fitting complementary "mold" which makes contact with it at several points simultaneously.

In three dimensions the easily imaginable (and perhaps only) ways of achieving more than  $3N-6$  contacts among  $N$  particles involve generating sizable fragments of perfect crystal, the simplest of which are the ten-atom fragments shown in Figs. 8(a) and 8(b). Each of these is made up of two tetrahedral and two octahedral voids; however, perfect octahedra have zero probability of being formed during a serial deposition on a small or amorphous seed<sup>14</sup> and, as was pointed out earlier, occur rarely or not at all in Finney's packing. One reason for the infrequency of their formation during the compacting process to which Finney's packing was subjected may be that they are bulky compared to other arrangements of six atoms (e.g., an octahedral void, which contains about  $0.13\sigma^3$  of empty space, can be collapsed into three tetrahedral voids sharing a common edge and having a total empty volume of  $0.08\sigma^3$ ). These numbers merely suggest that compression would tend to collapse isolated octahedral voids; to prove this would require comparing not only the internal volumes of the two six-atom configurations, but also the "interfacial" volume deficits or excesses they give rise to by being embedded in an amorphous matrix. In any case, it appears likely that the formation of redundant contacts during the compression of a serially deposited cluster is equivalent to the formation of crystalline regions, and that even the smallest of these yielding any redundant contacts, i.e., those of Figs. 8(a) and 8(b), are unlikely to be formed because of their complexity, and because they are probably bulkier *in situ* than other configurations of the same



number of atoms. Hence a three-dimensional hard-sphere packing should exhibit considerable resistance to homogeneously nucleated crystallization, and its mean coordination number at contact should remain 6.0 as long as it is amorphous.

In two dimensions homogeneous nucleation occurs easily, and attempts to produce dense random packings generally result in crystallization.<sup>15</sup> Various explanations may be offered, e.g., the simplicity of the minimal crystal fragment [Fig. 8(c)] allowing redundant contacts, and the fact that this fragment is the densest configuration of seven atoms. Aside from this, there are important geometric differences between the two- and three-dimensional cases, of which perhaps the most conspicuous is the ability of equilateral triangles to fill space contrasted with the inability of regular tetrahedra to do so. Finney<sup>3</sup> notes another difference, the equality in two dimensions, between the mean Voronoi coordination numbers of the amorphous and crystal structures, compared with their inequality in three dimensions.

#### ACKNOWLEDGMENTS

The author wishes to thank David Turnbull and Arthur Bienenstock for constant advice, encouragement, and inspiration, Joan Lewis for teaching the author how to use the IBM 7094 computer, and John Finney, Slade Cargill, and Ray Baughman for numerous and helpful discussions of their experimental work.

\*Work done partly under the auspices of the U.S. Atomic Energy Commission. Supported by the NSF (Contract Nos. GP2174 and GP7022).

<sup>†</sup>In partial fulfillment of the requirement for the Ph.D. degree.

<sup>1</sup>J. D. Bernal and J. Mason, *Nature* 188, 910 (1960).

<sup>2</sup>G. D. Scott, *Nature* 194, 956 (1962).

<sup>3</sup>J. L. Finney, *Proc. Roy. Soc. (London)* 319A, 479 (1970); 319A, 495 (1970).

<sup>4</sup>D. Turnbull and M. H. Cohen, *Nature* 203, 964 (1964).

<sup>5</sup>R. Hilsch, in *Non-Crystalline Solids*, edited by V. D. Frechette (Wiley, New York, 1960), pp. 348–373.

<sup>6</sup>H. S. Chen and D. Turnbull, *J. Chem. Phys.* 48, 2560 (1968).

<sup>7</sup>W. Klement, R. H. Willens, and P. Duwez, *Nature* 187, 869 (1960).

<sup>8</sup>P. Duwez, *Trans. Am. Soc. Metals* 60, 605 (1967).

<sup>9</sup>S. Mader, H. Widmer, F. M. d'Heurle, and A. S. Nowick, *Appl. Phys. Letters* 3, 201 (1963).

<sup>10</sup>G. S. Cargill, *J. Appl. Phys.* 41, 12 (1970); 41, 2248 (1970).

<sup>11</sup>This same algorithm was used by L. D. Norman and E. E. Maust, Jr., U.S. Bureau of Mines, College Park, Md., to build a small packing described by them in a paper presented at the May 1970 meeting of the Metallurgical Society of AIME, Las Vegas, Nevada.

<sup>12</sup>B. J. Alder (unpublished); and *Phys. Rev. Letters* 12, 317 (1964).

<sup>13</sup>F. J. Stillinger, *J. Comp. Phys.* 7, 367 (1971).

<sup>14</sup>This is because the last step in forming an octahedron must be the addition of an atom to the base of an Archimedean pyramid. Since the latter has one internal degree of freedom, its shape is determined by the matrix in which it is embedded, and, if the matrix is amorphous, there is no reason for the base to be exactly square as is required for completion of a perfect octahedron.

<sup>15</sup>J. L. Finney (private communication).

## Method of Isentropically Compressing Materials to Several Megabars\*

R. S. Hawke, D. E. Duerre, J. G. Huebel, H. Klapper, and D. J. Steinberg  
*Lawrence Livermore Laboratory, University of California, Livermore, California 94550*  
and

R. N. Keeler  
*Department of Applied Science, University of California, Davis, California 95616*  
(Received 8 December 1971)

This paper describes a new method of compressing materials up to pressures of several megabars. A high-intensity magnetic field, obtained by magnetic flux compression, is used to compress a sample contained in a metallic tube. The compression of the sample is slow enough to avoid the generation of shock waves which allows the process to be isentropic. This paper describes the apparatus and several experiments with Lucite samples. Evidence that Lucite was isentropically compressed to a specific volume of about 0.25 is included. The pressure reached is estimated to be ~4 Mbar.

#### INTRODUCTION

In the past, high pressures in materials have been attained by static high-pressure techniques and dynamic shock-wave techniques.<sup>1,2</sup> Static presses have been designed and operated to pressures in the vicinity of 0.5 to 1.0 Mbar, although above 100 kbar large uncertainties exist in the pressure scale. With shock-wave techniques it has been possible to attain pressures in the vicinity of 10 Mbar in stiff materials; however, the maximum obtainable pressure diminishes in more compressible materials. The equations of state and properties of highly compressible materials, particularly non-metals, are of considerable scientific interest. Therefore, it is appropriate to investigate alternative tech-

niques of coupling the high energy of an explosive to a sample in such a way that high pressures are reached without large temperature increases.

One such technique is the use of a magnetic field to transfer the energy of high explosives to containers and their samples,<sup>3-6</sup> and a considerable amount of technology already exists for magnetic flux compression.<sup>7-9</sup> Using magnetic flux compression, we have been able to attain pressures in the megabar range in a relatively compressible material. Furthermore, the rate of pressure change on the sample has been low enough that the compression has been shockless and essentially hydrostatic. Thus, the compression of the material has been isentropic, permitting a complete description of